Supporting Information

$[Ag_{71}(S\text{-}tBu)_{31}(Dppm)](SbF_6)_2$: an intermediate sized metalloid silver nanocluster containing a building block of Ag_{64}

Manman Zhou,‡ Yizheng Bao,‡ Shan Jin,* Shuaishuai Wen, Shuang Chen, Manzhou Zhu*

Institutes of Physical Science and Information Technology, Anhui University, Hefei, Anhui, 230601, P. R. China; Key Laboratory of Structure and Functional Regulation of Hybrid Materials (Anhui University), Ministry of Education, Hefei, 230601, P. R.

1.1 Chemicals Materials

Silver nitrate ($AgNO_3$, 99.0%, Sigma-Aldrich), Sodium borohydride ($NaBH_4$, 98%, Sigma-Aldrich), Sodium borodeuteride ($NaBD_4$, 98%, Sigma-Aldrich) bis-(diphenylphosphino)methane (Dppm, 98%), t-butyl mercaptan (97%, Sigma-Aldrich), Tetraphenylboron sodium ($NaBPh_4$, 98%), Sodium hexafluoroantimonate ($NaSbF_6$, 99%, Energy Chemical) methanol (CH_3OH, HPLC, Aldrich), Toluene (Tol, HPLC grade, Aldrich), n-hexane (Hex, HPLC grade, Aldrich), dichloromethane (CH_2Cl_2, HPLC grade, Aldrich). All reagents were used as received without further purification.

1.2 The Synthesis of $Ag_{71}(SR)_{31}(Dppm)(SbF_6)_2$

For the synthesis of nanocluster, 60 mg $AgNO_3$ was dissolved in 1 mL of H_2O, then added into 14 mL toluene. After this solution stirred for 10 min, 50 mg bis-(diphenylphosphino)methane and 50 ul t-butyl mercaptan were added together to the solution under vigorous stirring. The clear and transparent solution gradually turned milky white. 15 minutes later, a freshly prepared solution of 20 mg $NaBH_4$ (1 mL H_2O) was added. After 3-5 min, the color of the reaction solution turned to red. The reaction sustained for 5 h at room temperature. The crude product was spied dry then dissolved in 1 mL CH_2Cl_2. 30 mg $NaSbF_6$ in 3 mL CH_3OH was added to replace the anion of the cluster for easy crystallization. The precipitate washed several times with CH_3OH and H_2O. Red crystals were crystallized for CH_2Cl_2/hexane 2-3 days later. The yield is about 30% based on the Ag element for $Ag_{71}(SR)_{31}(Dppm)(SbF_6)_2$.

$Ag_{71}(SR)_{31}(Dppm)(BPh_4)_2$ was crystalized by adding $NaBPh_4$ to replace the anion of the cluster, which was further used for NMR measure.

1.3 Characterization

All UV/Vis absorption spectra of nanoclusters were recorded using an Agilent 8453. Thermo gravimetric analysis (TGA) was carried out on a thermo gravimetric analyzer (DTG-60H, Shimadzu Instruments, Inc.) with 5 mg of the nanocluster in a SiO_2 pan at a heating rate of 10 K min^{-1} from 323 K to 973 K. X-ray photoelectron spectroscopy (XPS) measurements were performed on a Thermo ESCALAB 250 configured with a mono chromated AlKα (1486.8 eV) 150W X-ray source, 0.5 mm circular spot size, a flood gun to counter charging effects, and the analysis chamber base pressure lower than 1 x 10^{-9} mbar, data were collected with FAT= 20 eV. Electrospray ionization time-of-flight mass spectrometry (ESI-TOF-MS) measurement was performed by MicrOTOF-QIII high-resolution mass spectrometer. The sample was directly infused into the chamber at 5μL/min. Nuclear magnetic resonance (NMR) analysis was performed on a Bruker Avance spectrometer operating at 400 MHz for NMR. CD_2Cl_2 was used as the solvent

to dissolve ~50 mg $[Ag_{71}(SR)_{31}(Dppm)][BPh_4]_2$ clusters; the residual solvent peak (i.e.,1H at 5.32 ppm) was used as reference.

1.4 Electrochemical measurements

Electrochemical measurements were performed with an electrochemical workstation (CHI700E) using a Pt working electrode (diameter 0.4 mm), a Pt wire counter electrode, and a Ag wire quasireference electrode in 0.1 MBu_4NPF_6-CH_2Cl_2. Prior to use, the working electrode was polished with 0.05 μm Al_2O_3 slurries and then cleaned by sonication in dilute CH_3CH_2OH and nanopure water successively. The electrolyte solution was deaerated with ultra-highpurity nitrogen for 30 min and blanketed under nitrogen atmosphere throughout the experimental procedure.

1.5 X-Ray Crystallography

The data collection for single crystal X-ray diffraction was carried out on Stoe Stadivari diffractometer under liquid nitrogen flow at 173 K, using graphite-monochromatized Cu Kα radiation (λ = 1.54186 Å). Data reductions and absorption corrections were performed using the SAINT and SADABS programs, respectively.

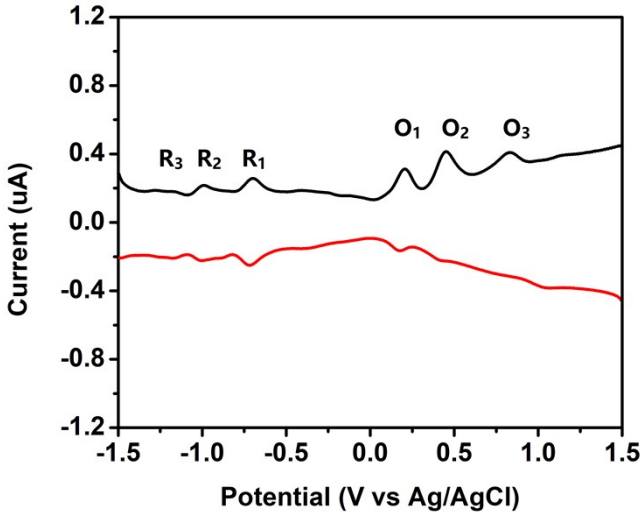

Figure S1. Differential pulse voltammogram of $[Ag_{71}(SR)_{31}(Dppm)](SbF_6)_2$ in CH_2Cl_2 in the low temperature environment formed by dry ice in acetonitrile.

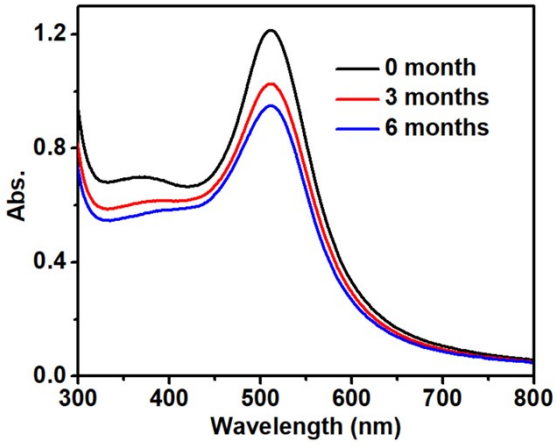

Figure S2. the UV-vis of $[Ag_{71}(SR)_{31}(Dppm)](SbF_6)_2$ stored in solid states for 0, 3 and 6 months.

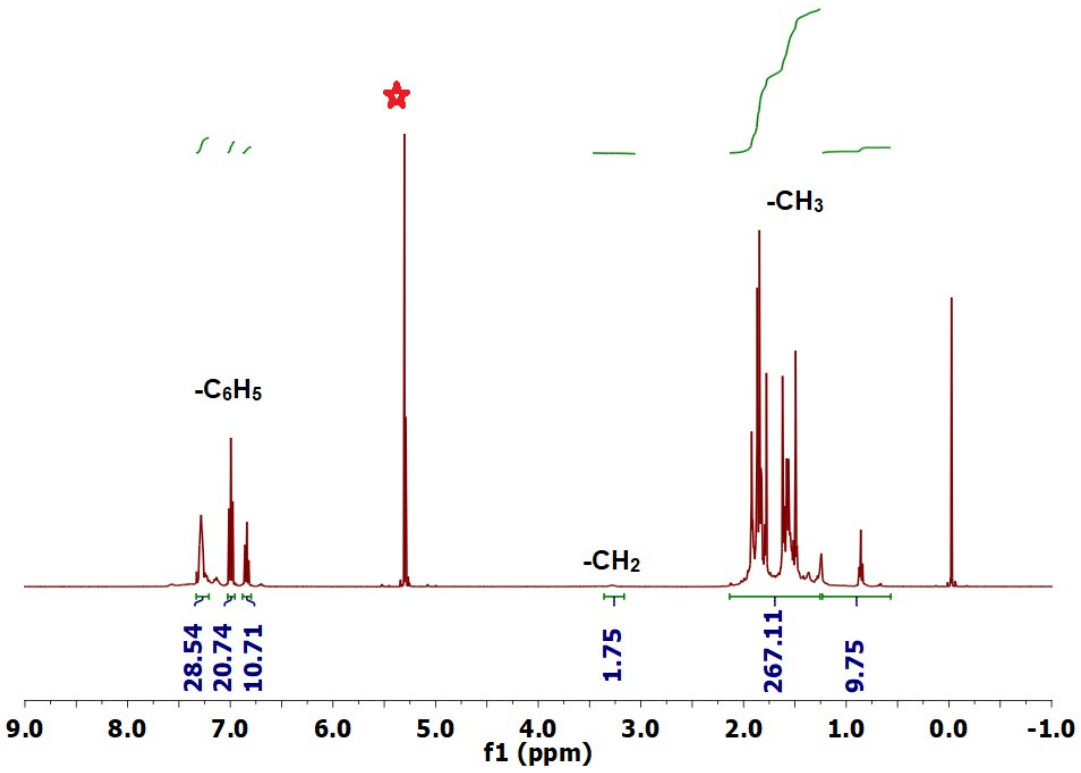

Figure S3. ^{1}HNMR spectra of the $[Ag_{71}(SR)_{31}(Dppm)][BPh_4]_2$ clusters dissolved in CD_2Cl_2. The residual solvent peak (i.e.,^{1}H at 5.32 ppm) was used as reference.

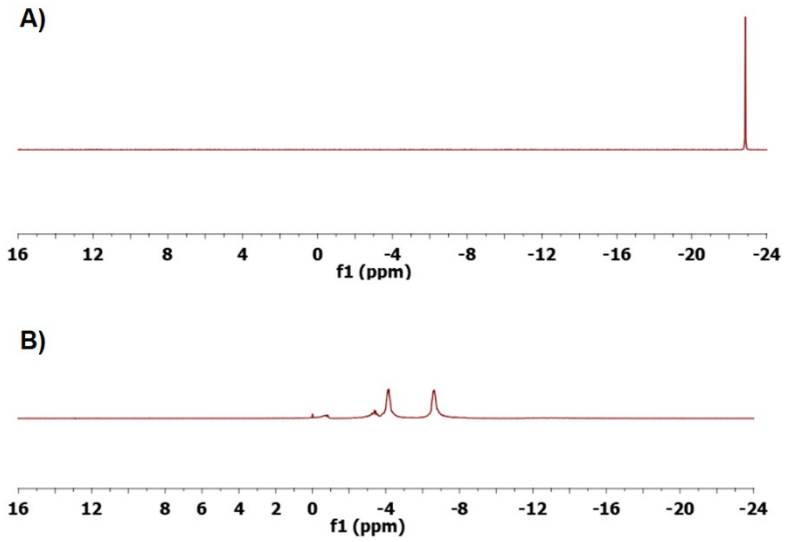

Figure S4. ^{31}PNMR spectra of the A) free Dppm and B) 50mg $[Ag_{71}(SR)_{31}(Dppm)][BPh_4]_2$ clusters dissolved in CD_2Cl_2.

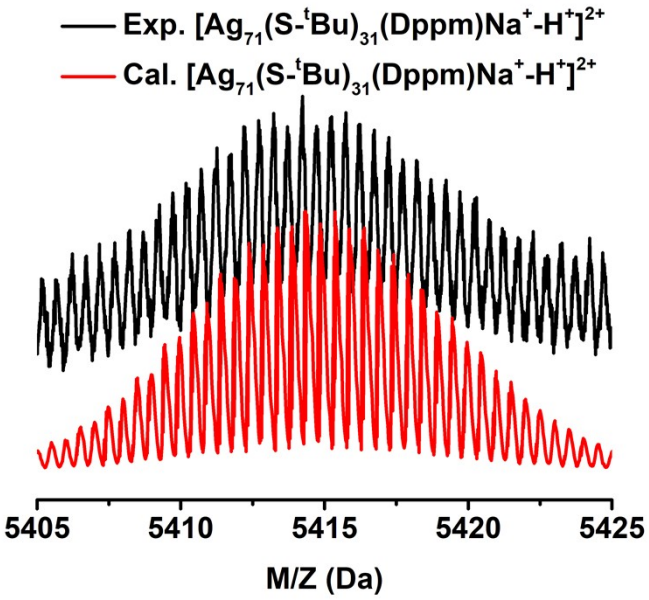

Figure S5. Comparison of the calculated and the experimental isotopic distributions of $[Ag_{71}(S\text{-}tBu)^{31}(Dppm)Na^{+}\text{-}H^{+}]^{2+}$

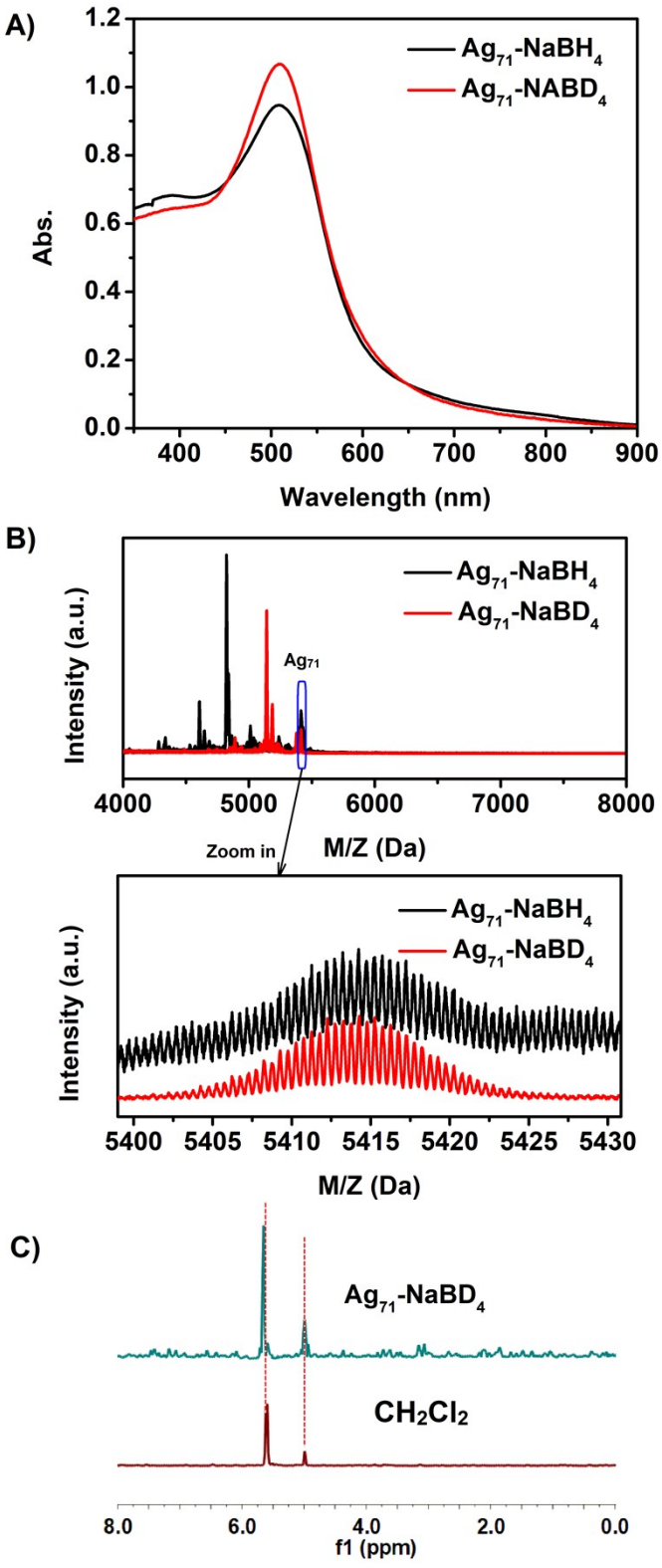

Figure S6. A) the UV-vis spectrum of $[Ag_{71}(SR)_{31}(Dppm)][BPh_4]_2$ synthesized via $NaBH_4$ and $NaBD_4$. B) the comparison of ESI-MS spectra between the products from $NaBH_4$ and $NaBD_4$; C) ^{2}HNMR spectra of the $[Ag_{71}(SR)_{31}(Dppm)][BPh_4]_2$ clusters dissolved in CH_2Cl_2 and the purified CH_2Cl_2 . The result indicated there was no additional signal in spectra, meaning that no D atom was incorporated into Ag_{71}-D, ruling out the existence of hydrides (H^-) in the structure.

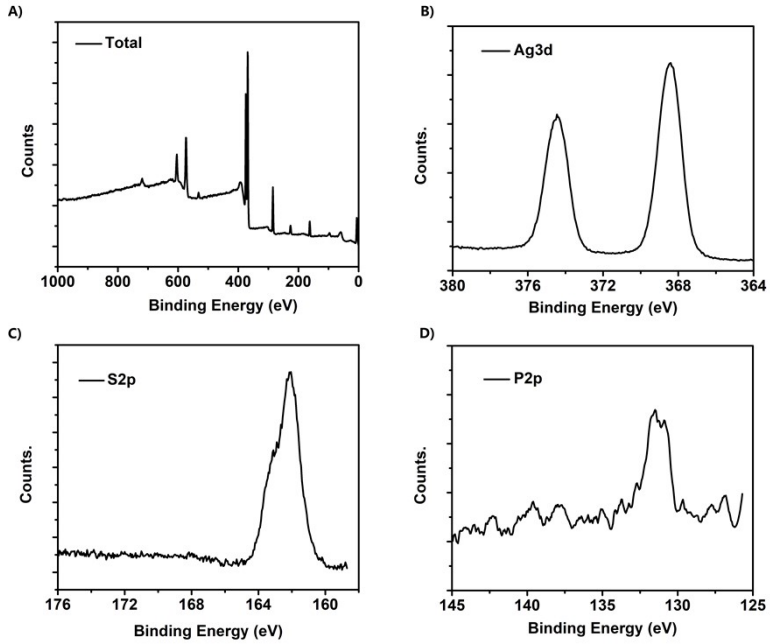

Figure S7. X-ray photoelectron spectroscopy (XPS) data of $[Ag_{71}(SR)_{31}(Dppm)](SbF_6)_2$.

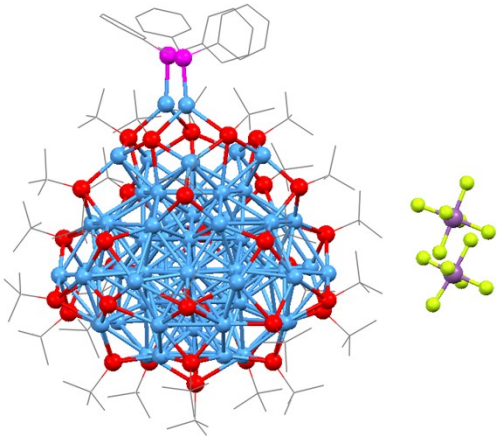

Figure S8. The structure of $[Ag_{71}(SR)_{31}(Dppm)](SbF_6)_2$ Color Labels: light blue = Ag; red = S; pink = P; purple=Sb; yellow-green = F; gray = C, .

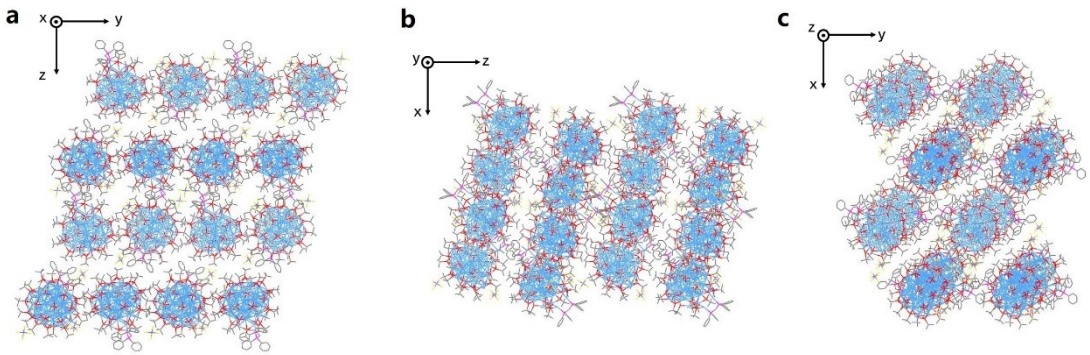

Figure S9. The packing model of $[Ag_{71}(SR)_{31}(Dppm)](SbF_6)_2$ from different views. Color Labels: light blue = Ag; red = S; pink = P; gray = C.

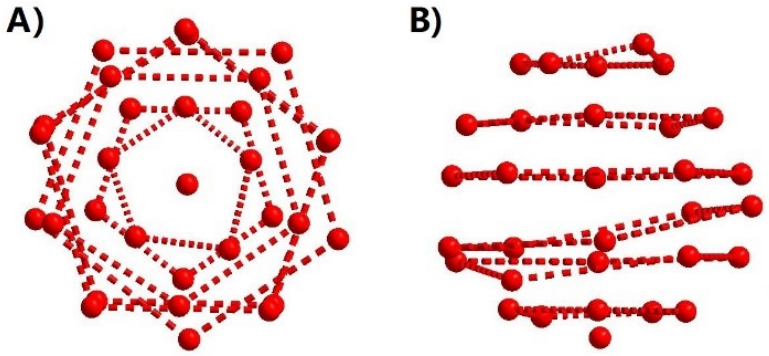

Figure S10. The arrangement of thiol ligands in the $[Ag_{71}(SR)_{31}(Dppm)]^{2+}$. Five thiol ligands in each layer could form a pentagon. There are five twisted pentagons and one sole thiol ligand. The arrangement was rarely observed in the reported nanoclusters.

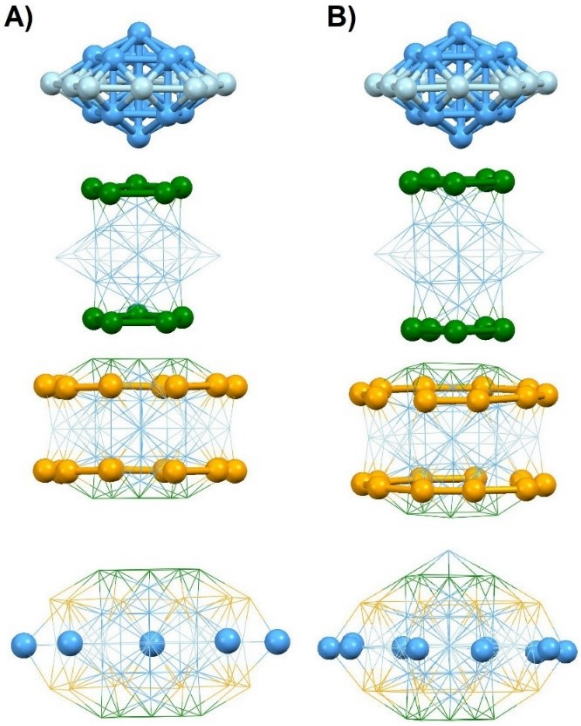

Figure S11. the comparison of A) Ag_{58} core structure of the $Ag_{78}(iPrPhS)_{30}(dppm)_{10}Cl_{10}]^{4+}$ and B) Ag_{64} core structure of $[Ag_{71}(SR)_{31}(Dppm)]^{2+}$.

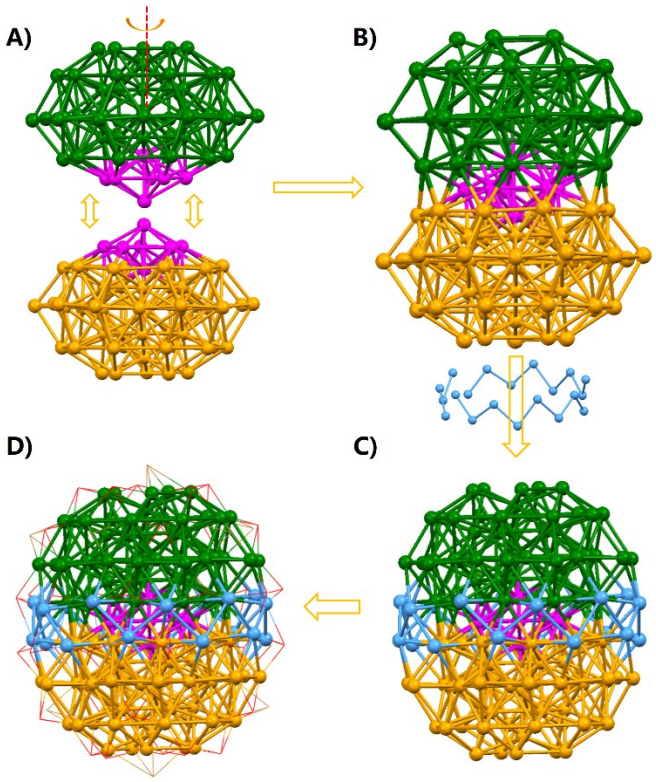

Figure S12. the structural analysis of Ag_{141} via Ag_{64} unit assembled, which the Ag_{64} structure could be observed in $Ag_{71}(S\text{-}^{t}Bu)_{31}(Dppm)](SbF_6)_2$.

Table 1. Crystal data and structure refinement for Ag71.

Empirical formula	$C_{149}H_{301}Ag_{71}F_{12}P_2S_{31}Sb_2$
Formula weight	11278.95
Temperature/K	173(2)
Crystal system	triclinic
Space group	P-1
a/Å	24.7024(15)
b/Å	33.182(2)
c/Å	38.8512(18)
α/°	102.791(3)
β/°	103.733(2)
γ/°	90.602(3)
Volume/Å^3	30100(3)

Z	4
Radiation	CuKα (λ = 1.54186)
2Θ range for data collection/°	2.736 to 135
Index ranges	$-29 \leq h \leq 29$, $-39 \leq k \leq 38$, $-43 \leq l \leq 46$
Reflections collected	363852
Independent reflections	108067 [R_{int} = 0.0721, R_{sigma} = 0.1060]
Data/restraints/parameters	108067/19/4940
Goodness-of-fit on F^2	1.079
Final R indexes [I>=2σ (I)]	R_1 = 0.0458, wR_2 = 0.0805
Final R indexes [all data]	R_1 = 0.0676, wR_2 = 0.0941
Largest diff. peak/hole / e $Å^{-3}$	4.18/-4.65